Indian J. Phys. **70B** (5), 397–407 (1996)

IJP B
- an international journal

Optical properties of Er^{3+} doped fluoroborate glasses

Brajesh Sharma, D K Rai and S B Rai
Department of Physics, Banaras Hindu University,
Varanasi-221 005, India

Received 21 March 1996, accepted 20 June 1996

Abstract : A detailed study of the physical, absorption and fluorescence properties of six Er^{3+} doped fluoroborate glasses at 300 K and 77 K has been carried out. From the experimental values of the oscillator strengths the Judd-Ofelt intensity parameters have been obtained. The transition probabilities, radiative branching ratios and the stimulated emission cross section for the different transitions have also been calculated using these parameters. From these studies it is concluded that the presence of Al in fluoroborate galss show better optical characteristics. The transition $^4S_{3/2} \rightarrow {}^4I_{15/2}$ show largest stimulated cross section and fluorescence yield.

Keywords : Fluorescence, Fluoroborate glass, Judd-Ofelt parameters

PACS No. : 42.70.Ce

1. Introduction

There are a number of characteristics which distinguish glass from other solid laser host materials. Their isotropic character, possibility of even heavy doping with excellent uniformity and the strong sharp fluorescence lines observed in rare earth doped glasses make them host materials of choice for optically pumped laser devices.

Over the past few years, a great deal of work has been done by us in the development and characterisation of rare earth doped calibo, silicate and fluorophosphate glasses to understand their fluorescence behaviour [1–3]. Recently another type of glass material which contains borate at the place of phosphate has been developed and the emission and absorption characteristics of several rare earth doped ions have been studied. It has been marked that the fluoroborate glass is very similar to fluorophosphate in properties and is more stable over a wide compositional range and may be useful for different purposes. In the present paper we have studied the physical, optical emission and absorption characteristics of Er^{3+} doped fluoroborate glass. We have selected Er^{3+} for our

study since Er^{3+} is well known lasing material and lases at 1.54 μm when it is doped in glass and at 2.8, 1.6 and 0.85 μm respectively when doped in crystalline solid [4]. Our basic idea is to see the emission and absorption characteristics of Er^{3+} in new fluoroborate lattice and compare it with fluorophosphate lattice.

2. Preparation of the glass

Six Er^{3+} doped fluoroborate glasses with alkali (Na, Li) and Al fluoride in separate and in mixed forms were prepared with compositions (mole %) $2ErF_3 + 78H_3BO_3 + 10Na_2CO_3 + 10RF$ where RF = NaF, LiF, AlF_3, NaF + AlF_3, LiF + AlF_3 and NaF + LiF. The nomenclature (BNa glass, BNaAl glass *etc.*) describes the presence of single and coupled forms of alkali with Al in the ternary systems studied. H_3BO_3, Na_2CO_3, LiF and AlF_3 were of BDH make with 99% purity. ErF_3 was obtained from Aldrich company with a stated purity of 99.9%. Each chemical batch is homogeneously mixed up by powdering well in an agate mortar before melting them at temperature between 900–1000°C in a platinum crucible in an electric furnace. The melts were quenched in between two smooth surfaced and polished plates (one of which acts as a cast) to obtain smooth, flat surfaces on the glass synthesized. The glasses thus obtained are in the form of circular discs having a uniform thickness of 0.32 cm. The glasses are preserved in containers filled up with liquid paraphin to avoid possible damage.

2.1. Experimental measurements :

The density of the glasses have been measured by the application of Archimede's principle using xylene as the immersion liquid and is found in the range of 2.5 ± 0.2 (gm/cm^3) in different cases. The refractive indices of these glasses have been determined at $\lambda = 589.3$ nm using an Abbe refractometer with monobromonaphthalene as the contact layer between the sample and the prism of the refractometer. For all the glasses the refractive index (n) values are very similar ~ 1.48 ± 0.01.

The absorption spectra (800–200 nm) of fluoroborate glasses were measured using a Cary (model) 2390 UV-VIS-NIR spectrophotometer. For fluorescence measurement we have used the different lines of an Ar^+ laser as excitation lines. It is noted that though the fluorescence appears for all Ar^+ lines, the fluorescence yield is maximum for 457.9 nm. A 20 mW output power of 457.9 nm was used to excite the fluorescence. The dispersed fluorescence were recorded using a 0.5 m Spex monochromator coupled to a double pen X-Y chart recorder. The atomic lines from a Fe–Ne hollow cathode lamp superposed on fluorescence was used for wavelength calibration. The fluorescence spectra were recorded both at room temperature and at liquid N_2 temperature. For recording the spectra at 77 K, a double-wall cell of glass was fabricated. The glass was suspended in the inner cavity of the cell with the help of a rod and screw arrangement so that its flat surface is perpendicular to the laser beam. The rod dipped in the liquid N_2 served as finger tip.

3. Results and discussion

3.1. Absorption spectrum and Judd-Ofelt parameters of Er^{3+} :

The absorption spectrum of Er^{3+} doped BAl fluoroborate glass in the UV visible NIR region (800–200 nm) at room temperature is shown in Figure 1. Spectrum very much similar to this, have been observed in the case of other glasses. All these spectra show ten descrete lines in the above wavelength region due to transitions between energy levels associated with the 4*f* shell. The intensity of the individual lines however vary from one spectrum to the other. These transitions though normally dipole forbidden become allowed in the glassy

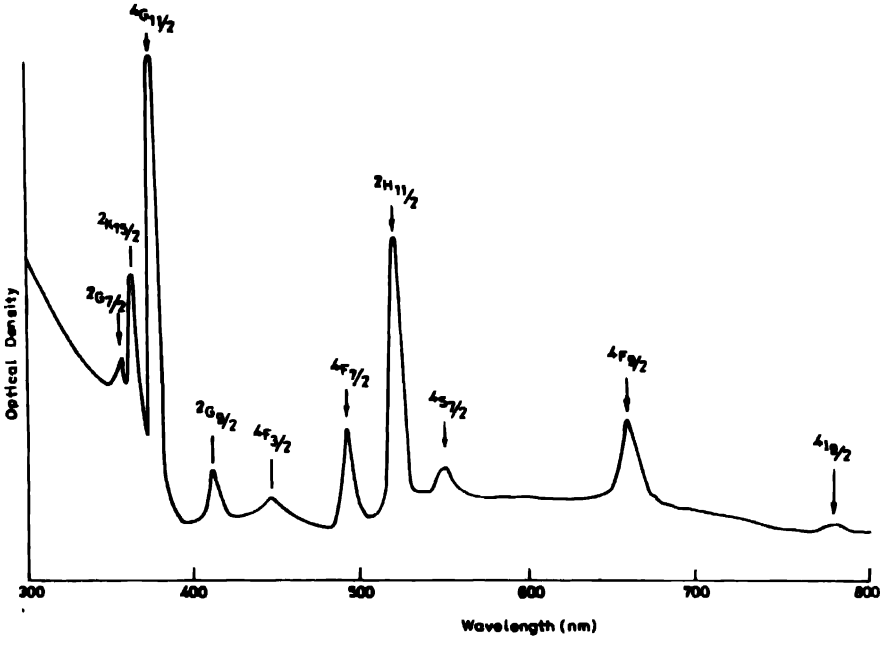

Figure 1. UV-visible absorption spectrum of Er^{3+}-doped BAl glass

host due to vibronic interaction or through admixture of odd electronic wave functions. The lines could be easily assigned on the basis of the analysis of the absorption of Er^{3+} in other glass hosts. The line wavenumbers and the assignments for the different glass hosts are given in Table 1. From the absorption spectrum it is clear that $^4G_{11/2} \leftarrow {}^4I_{15/2}$ transition and $^2H_{11/2} \leftarrow {}^4I_{15/2}$ transition appear with the largest intensity in all cases. The transition ending on the $^4G_{11/2}$ level is hypersensitive to the host constitution and is of maximum intensity in the BAl type glass. The intensity of this transition in the other combinations follows the trend BAl > BNaAl > BLiAl > BLi > BLiAl > BNaLi. A similar intensity pattern is followed by the $^2H_{11/2} \leftarrow {}^4I_{15/2}$, $^2K_{15/2} \leftarrow {}^4I_{15/2}$ *etc.* transitions also. The intensity of the spectral lines are smaller in the glasses containing Li. The transition $^2G_{7/2} \leftarrow {}^4I_{15/2}$ appears only with very weak intensity and is almost missing in the glass containing both Na and Al. The $^2I_{9/2} \leftarrow {}^4I_{15/2}$ transition appears with a large spectral width in all the glasses whereas the $^2F_{9/2} \leftarrow {}^4I_{15/2}$ transition is specially broad in glasses containing Li.

Table 1. Measured ($f_m \times 10^{-6}$) and calculated ($f_c \times 10^{-6}$) oscillator strengths of Er^{3+} doped fluoroborate glasses at room temperature. All transitions from the $^4I_{15/2}$ level to the level indicated.

Level	$^4I_{9/2}$	$^4F_{9/2}$	$^4S_{3/2}$	$^2H^a_{11/2}$	$^4F_{7/2}$	$^4F_{3/2}$	$^2G_{9/2}$	$^2G^a_{11/2}$	$^2K_{15/2}$	$^2G_{7/2}$
Energy (cm^{-1})	12500	15300	18400	19200	20500	22600	24600	26400	27600	28000
$\|\|U^2\|\|^2$	0	0	0	0.713	0	0	0	0.918	0.022	0
$\|\|U^4\|\|^2$	0.173	0.535	0	0.413	0.147	0	0.019	0.526	0.004	0.017
$\|\|U^6\|\|^2$	0.010	0.462	0.221	0.093	0.627	0.127	0.226	0.117	0.076	0.116
BNa glass										
f_m	0.251	1.68	0.381	4.91	0.486	0.295	0.286	5.860	2.120	1.120
	0.19*	1.39*	0.35*	2.54*	1.10*	0.22*		5.45*		
	0.66*	4.2**	0.94**	7.92**	3 8**					
f_c	0.312	1.97	0.402	4.61	0.458	0.213	0.275	5.62	2.33	1.21
BLi glass										
f_m	0.265	1.63	0.285	3.92	0.472	0.262	0.159	4.92	1.92	0.961
f_c	0.301	1.68	0.296	3.52	0.484	0.258	0.176	4.92	1.88	0.921
BAl glass										
f_m	0.302	2.32	0.311	5.12	0.562	0.252	0.291	6.01	2.13	1.21
f_c	0.495	2.67	0.352	5.63	0.559	0.265	0.261	6.13	2.00	1.01
BNaAl glass										
f_m	0.286	1.85	0.262	3.82	0.352	0.265	0.211	4.85	1.86	–
f_c	0.395	1.73	0.280	3.92	0.365	0.263	0.225	4.86	1.92	–
BLiAl glass										
f_m	0.399	1.95	0.292	3.78	0.395	0.159	0.101	4.28	1.53	0.861
f_c	0.532	2.01	0.10	4.0	0.401	0.201	0.111	4.31	1.91	0.861
BNaLi glass										
f_m	0.253	1.63	0.371	3.92	0.385	0.282	0.212	3.91	2.01	0.621
f_c	0.285	1.85	0.382	3.71	0.376	0.325	0.314	4.02	2.10	0.651

Note : * = ($f_m \times 10^{-6}$) in BaF_2–ThF_4 fluoride glass reported by Yeh *et al* (13). ** = ($f_m \times 10^{-6}$) in fluorophosphate glasses reported by Ranga Reddy *et al* (15).
a = Hyper sensitive transition for Er^{3+}.

Table 2. A comparison of Judd-Ofelt intensity parameters for the Er^{3+}-doped fluoroborate glass with the heavy metal fluoride, chloro and fluorophosphate glasses.

Glasses	Judd-Ofelt parameters			Quality factor (Ω_4/Ω_6)	References
	Ω_2 (10^{+20} cm^2)	Ω_4 (10^{+20} cm^2)	Ω_6 (10^{+20} cm^2)		
BNa glass	3.03	2.0	1.12	1.780	Present work
BLi glass	2.51	1.69	1.02	1.650	"
BAl glass	3.41	2.41	1.63	1.470	"
BNaAl glass	2.38	1.64	0.97	1.690	"
BLiAl glass	2.1	2.18	0.99	2.202	"
BNaLi glass	2.19	1.9	1.01	1.881	"
$57ZrF_4$–$34BaF_2$–$4AlF_3$–$3NaF_3$–$2ErF_3$	3.26	1.85	1.14	–	[13]
$19BaF_2$–$27ZnF_2$–$5YbF_3$–$27ThF_3$–$21LuF_3$–$1ErF_3$	2.44	1.55	1.18	–	[13]
$30BaF_2$–$20ZnF_2$–$30InF_3$–$84YbF_3$–$10ThF_3$–$2ErF_3$	2.19	1.52	0.91	–	[13]
$48(NaPO_3)_6$–$20BaCl_2$–$10ZnCl_2$–$20LiCl$–$2ErCl_3$	2.39	1.43	0.85	–	[14]
$50(NaPO_3)_6$–$18BaF_2$–$10ZnF_2$–$20LiF$–$2ErF_3$	5.33	4.713	2.62	–	[15]

A comparison of intensity of the fluorescence lines in Er^{3+} doped fluoroborate glass with the corresponding lines in Er^{3+} doped fluoro and chlorophosphate glasses gives interesting results. Thus while in fluorophosphate glasses the $^4I_{9/2} \leftarrow {}^4I_{15/2}$ transition is more intense and broadened than the $^4F_{9/2} \leftarrow {}^4I_{15/2}$ transition, the reverse holds true in the case of fluoroborate glasses. The lines have similar intensity for Er^{3+} in fluoroborate and in chlorophosphate glasses. The Judd-Ofelt [5,6] intensity parameters Ω_λ (where $\lambda = 2$, 4 and 6) are sensitive to the host due to their dependence on the site symmetry, radial integral and the energy difference between the $4f$ levels and the close-lying, perturbing configurations. Therefore it was thought worthwhile to calculate the intensity parameters Ω_λ for Er^{3+} doped fluoroborate glasses from the experimentally measured electric dipole oscillator strength given by the Reisfeld [7] formula as

$$P = 4.318 \times 10^{-9} \int \sigma(\nu) d\nu \qquad (1)$$

and the calculated matrix elements (see Carnall *et al* [8]) between the various levels of the rare earth ion (Er^{3+}). The intensity parameters thus obtained are tabulated in Table 2. It is found that the Judd-Ofelt parameter Ω_λ is maximum for the Al (only) containing borate glass as compared to the other five fluoroborate lattices. Even with Al, it is smaller compared to the value in fluorophosphate but larger compared to chlorophosphate glasses. Its value is very much similar to heavy metal fluoride glasses. Ω_λ parameters follow the trend $\Omega_2 > \Omega_4 > \Omega_6$ which is identical to other glasses. The measured and calculated oscillator strength for different transitions from $^4I_{15/2}$ in the six fluoroborate glasses are given in Table 1.

3.2. *Fluorescence spectrum of Er^{3+} doped fluoroborate glass :*

The fluorescence spectrum of BAl glass out of six Er^{3+} doped fluoroborate glasses at room temperature and at liquid N_2 temperature is shown in Figure 2. The spectrum in the spectral

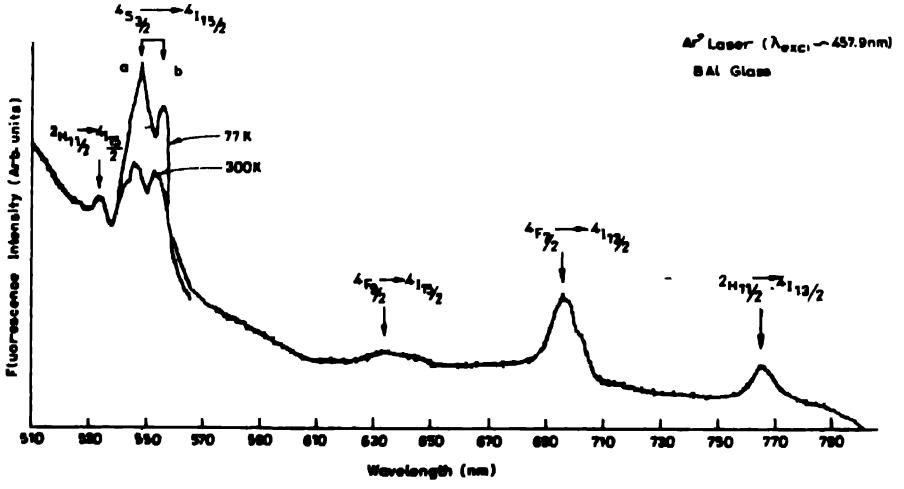

Figure 2. Fluorescence spectrum of Er^{3+}-doped BAl glass.

Table 3. Transition probability (A) total transition probability (A_T) and branching ratio of Er^{3+} (2 mol%) doped fluoroborate glass.

Transition	Energy	BNa glass		BLi glass		BAl glass		BNaAl glass		BLiAl glass		BNaLi glass	
	(cm^{-1})	A	β%	A	β%	A	β%	A	β%	A	β%	A	β%
$^7H_{11/2} \rightarrow$													
$^4S_{5/2}$	754	1.000	0.002	1.000	0.002	2	0.004	1	0.002	1	0.003	1	0.003
$^4F_{9/2}$	3882	124	0.297	104	0.297	141	0.290	98	0.293	88	0.259	91	0.273
$^4I_{9/2}$	8740	1354	3.253	1103	3.224	1080	3.450	1107	3.315	1090	3.219	1096	8.291
$^4I_{11/2}$	8991	553	1.328	489	1.340	670	1.378	452	1.353	537	1.586	492	1.477
$^4I_{13/2}$	12625	906	2.177	782	2.235	1124	2.312	744	2.228	845	2.495	949	2.840
$^4I_{15/2}$	19120	38675	92.94	32466	92 8	44982	92.557	30982	92.804	31294	92.435	30673	92.105
A_T		41613		34985		48599		33384		33855		33302	
$^4S_{3/2} \rightarrow$													
$^4F_{9/2}$	3128	4	0.031	3	0.026	6	0.032	3	0.027	3	0.026	3	0.026
$^4I_{9/2}$	5986	508	4.040	451	3.949	696	3.820	432	3.977	486	4.363	257	2.311
$^4I_{11/2}$	8237	288	2.294	260	2 277	412	2.261	248	2.283	260	2.324	261	2.347
$^4I_{13/2}$	11871	3447	27.46	3139	27.49	5016	27.531	2985	27.481	3046	27.350	3108	27.947
$^4I_{15/2}$	18366	8307	66.17	7505	66.26	12089	66.353	7194	66.230	7342	85.924	7491	67.305
A_T		12554		11418		18219		10862		11137		11120	

Table 3. *(Cont'd.)*.

Transition	Energy	BNa glass		BLi glass		BAl glass		BNaAl glass		BLiAl glass		BNaLi glass	
	(cm^{-1})	A	β%	A	β%	A	β%	A	β%	A	β%	A	β%
$^4F_{9/2} \rightarrow$													
$^4I_{9/2}$	2858	20	0.148	16	0.136	22	0.128	16	0.141	14	0.101	16	6.119
$^4I_{11/2}$	5109	474	3.524	472	4.033	532	3.090	470	4.161	450	3.278	460	3.658
$^4I_{13/2}$	8743	621	4.617	533	4.555	778	4 528	514	4.551	631	4.597	573	4.557
$^4I_{15/2}$	15238	12333	91.70	10680	91.27	15848	92.246	10294	91.145	12631	92.022	11526	91.665
A_T		13448		11701		17180		11294		13726		12574	
$^4F_{7/2} \rightarrow$													
$^2H_{11/2}$	1378	6	0.018	5	0.017	6	0.014	7	0.025	5	0.016	5	0.016
$^4S_{9/2}$	2132	1	0.003	1	0.003	2	0 004	1	0.003	1	0.003	1	0.003
$^4F_{9/2}$	5260	49	0.152	41	0.144	59	0.137	40	0.147	40	0.147	43	0.145
$^4I_{9/2}$	8118	1061	3.307	942	3 330	1453	3.392	901	3.320	981	3.141	958	3.327
$^4I_{11/2}$	10309	2192	0.832	1887	6.671	2459	5 741	1818	5.700	2258	7.262	2050	6.928
$^4I_{13/2}$	14003	5137	10 01	4341	15.35	6191	14 455	4213	15,528	5600	17.932	4880	16.493
$^4I_{15/2}$	20498	23637	73.69	21069	74.5	32058	76.253	20151	74.272	22327	71.496	21651	73.174
A_T		32083		28286		42428		27131		31228		29588	

region 790–510 nm shows five lines. The fluorescence intensity is larger at liquid N_2 temperature. The fluorescence peak at 550 nm ascribed to $^4S_{3/2} \rightarrow {}^4I_{15/2}$ transition is much stronger compareed to the other fluorescence peaks. $^4S_{3/2}$ level is known to be the upper level of the lasing transition in Er^{3+}. The $^4S_{3/2} \rightarrow {}^4I_{15/2}$ peak shows two components (*a* and *b*) of nearly equal intensity in all the borate hosts except in the glasses containing Al and Na along with *B* where the components with lower frequency has larger intensity. The other lines observed are ascribed to $^2H_{11/2} \rightarrow {}^4I_{15/2}$ (533.5 nm), $^4F_{9/2} \rightarrow {}^4I_{15/2}$ (638.6 nm), $^4F_{7/2} \rightarrow {}^4I_{13/2}$ (693.0 nm) and $^2H_{11/2} \rightarrow {}^4I_{13/2}$ (768.8 nm).

4. Radiative properties of Er^{3+} doped fluoroborate glasses

We have also calculated the transition probability, total transition probability and branching ratio for the different excited levels of Er^{3+} involved in the fluoroscence lines. The Judd-Ofelt parameters along with the reduced matrix element $\|U^\lambda\|$ previously reported by Carnall *et al* [9] have been utilized to calculate these parameters. The transition probability for a transition $j \rightarrow j'$ is given as

$$A(j,j') = 64\pi^4 e^2 \nu^3 / 3h(2j+1)\left[n(n^2+2)^2/9\right] \times S_{ed} \tag{2}$$

where j' and j are the J values of the ground and excited levels, ν is the transition frequency (cm^{-1}) and other factors have their usual meanings. The total transition probability $A_T(j,j')$ is given $\sum_{j'} A(j,j')$ *i.e.* the sum of the probabilities for all possible transitions starting from that level. The inverse of the total transition probability term gives us the radiative lifetime of that level. The branching ratio

$$\beta[(S,L,J);(S',L',J')] = \frac{A[(S,L,J);\ (S',L',J']}{\sum_{S',L',J'} A[(S,L,J);\ (S',L',J']} \tag{3}$$

where the sum is overall the terms in the manifolds. In Table 3 we have given the transition probability (A), total transition probability (A_T) and the branching ratio ($\beta\%$) of the observed emission states for all the glasses studied. Figure 3 depicts the branching ratio values for observed fluorescence transitions of Er^{3+} in fluoroborate glasses. Following the method of Weber *et al* [10], the stimulated emission cross section σ_p^E which controls the lasing efficiency of a particular energy level in a glass host is given by

$$\sigma_p^E(\Delta\lambda) = A(S,L,J \rightarrow S',L',J') / 8\pi^2 c n^2 \nu^4, \tag{4}$$

The stimulated emission cross section for the five transitions seen in the six fluoroborate glasses are tabulated in Table 4. From this Table it is clear that the emission cross section is maximum for the $^4S_{3/2} \rightarrow {}^4I_{15/2}$ transition in the BAl glass. In order to maximise the value of cross section we have to adjust Ω_λ and $\Delta\lambda$, the two terms which are glass composition dependent. To get maximum intensity, it is also essential to maximise the branching ratio for the particular transition. The fluorescence branching ratios are independent of Ω_2 and

can be expressed in terms of the ratio Ω_4/Ω_6, since Ω_4 and Ω_6 exhibit similar dependences on composition. It is seen that the variation in the values of $\beta\%$ with compositional changes are small [11,12].

Table 4. Fluorescence lines wevelength (λ), half width at full maximum ($\Delta\lambda$) and stimulated emission cross section ($\sigma_p^E \times 10^{20}$) values of Ar^+ laser (457.9 nm) excited Er^{3+} doped fluoroborate glasses.

Transition		BNa glass	BLi glass	BAl glass	BNaAl glass	BLiAl glass	BNaAl glass
$^2H_{11/2} \rightarrow {}^4I_{15/2}$	λ (nm)	.533.5	534.1	533.0	534.0	534.0	532 5
	$\Delta\lambda$ (nm)	8	9	8.5	7	6	7
	$\sigma_p^E \times 10^{20}$ cm^2	2.34	1.75	2.26	2.36	2.53	2.10
$^4S^{[a]}_{3/2} \rightarrow {}^4I_{15/2}$	λ (nm)	545.3	546.4	545.2	546.0	546.0	544.9
	$\Delta\lambda$ (nm)	21	20	21	20	19	20
	$\sigma_p^E \times 10^{20}$ cm^2	20.97	20.16	30.37	21.10	20.45	19.66
$^4S^{[b]}_{3/2} \rightarrow {}^4I_{15/2}$	λ (nm)	552.8	553.9	553.0	553.0	554.0	554.0
	$\Delta\lambda$ (nm)	18.4	18	18	19	16	17
	$\sigma_p^E \times 10^{20}$ cm^2	25 52	23.36	37.75	25.32	25.67	24 07
$^4F_{9/2} \rightarrow {}^4I_{15/2}$	λ (nm)	638 6	638.6	638.4	638.0	638.2	639.1
	$\Delta\lambda$ (nm)	57 5	58	56	56	58	56
	$\sigma_p^E \times 10^{20}$ cm^2	2.13	1.83	2 80	2 00	2.15	1.93
$^4F_{7/2} \rightarrow {}^4I_{13/2}$	λ (nm)	6 93.3	694.4	693.9	693.5	694.5	694.0
	$\Delta\lambda$ (nm)	21	21	20	22	21	20
	$\sigma_p^E \times 10^{20}$ cm^2	3 38	2.87	4 28	2.91	3 69	3.37
$^2H_{11/2} \rightarrow {}^4I_{13/2}$	λ (nm)	768.8	769 8	769.0	769 1	768 1	768 0
	$\Delta\lambda$ (nm)	6	6.5	8	7	7	8
	$\sigma_p^E \times 10^{20}$ cm^2	3.108	3.09	4 525	3 01	2 41	3.12

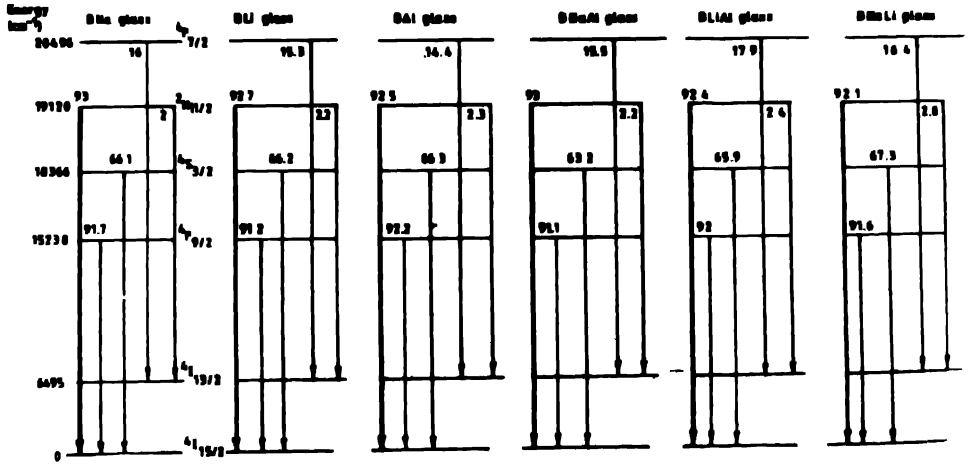

Figure 3. Energy level diagrams for fluorescence transitions of Er^{3+} in fluoroborate glasses. The numerical values correspond to branching ratio ($\beta\%$) and bold line indicates the maximum value of $\beta\%$.

In summary, based on different physical, absorption and fluorescence properties of a new family of fluoroborate glasses, it is seen that presence of Al in the fluoroborate glass composition makes this glass to have a superior optical characteristics. It shows larger stimulated emission cross section, fluorescence yield for $^4S_{3/2} \rightarrow {}^4I_{15/2}$ transition, a transition corresponding to which lasing has already been reported. Our results also confirm the suitability of the Judd-Ofelt theory for characterizing the optical properties of such glasses.

Acknowledgments

Authors are grateful to the Council of Scientific and Industrial Research and Department of Science and Technology, Government of India for financial assistance.

References

[1] Brajesh Sharma, J Vipin Prasad, S B Rai and D K Rai *Solid State Commun.* **93** 623 (1995)

[2] V N Rai, L B Tiwari, S N Thakur and D K Rai *Pramana* **19** 579 (1982)

[3] Brajesh Sharma, S B Rai, D K Rai and S Buddhudu *Indian J Engg. Mater. Sci.* **2** 297 (1995)

[4] M J Weber *Meth. of Exp. Phys.* **15A** 167 (1979)

[5] B R Judd *Phys. Rev.* **127** 750 (1962)

[6] G S Ofelt *J. Chem. Phys.* **37** 511 (1962)

[7] R Reisfeld *Struct. Bonding* **22** 124 (1975)

[8] W I Carnall, P R Fields and K Rajnak *J. Chem. Phys.* **49** 4412 (1968)

[9] W I Carnall, H Grosswhite and H M Grosswhite *Energy Level Structure and Transition Probabilities of the Trivalent Lanthanides in LaF_3.* (Argonne National Lab, USA) (1978)

[10] M J Weber *Hand Book on the Physics and Chemistry of Rare Earths* (Amsterdam : North Holland Publications) (1979)

[11] M J Weber, R A Saroyan and R C Ropp *J. Non-Cryst. Solids* **44** 148 (1981)

[12] C K Jorgenson and B R Judd *J. Mol. Phys.* **8** 281 (1964)

[13] D C Yeh, R R Petrin, W A Sibley, V Madigou, J L Adam and M J Suscavage *Phys. Rev.* **39** 80 (1989)

[14] K Subramanyam Naidu and S Buddhudu *J. Mater. Sci. Letts* **18** 299 (1992)

[15] A V Ranga Reddy, K Annapurna, G Amarnath, A S Jacob, A Suresh Kumar and S Buddhudu *Ferroelectrics Letts.* **14** 145 (1992)